

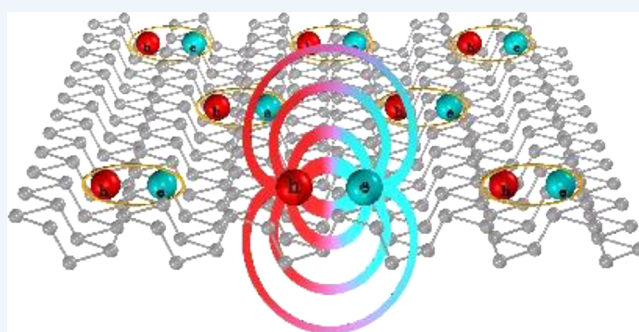
Highly Enhanced Many-Body Interactions in Anisotropic 2D Semiconductors

Ankur Sharma,[†] Han Yan,[†] Linglong Zhang,^{†,‡} Xueqian Sun,[†] Boqing Liu,[†] and Yuerui Lu^{*,†}

[†]Research School of Engineering, College of Engineering and Computer Science, The Australian National University, Canberra, Australian Capital Territory 2601, Australia

[‡]National Laboratory of Solid State Microstructures, Collaborative Innovation Center of Advanced Microstructures, School of Electronic Science and Engineering, Nanjing University, Nanjing 210093, People's Republic of China

ABSTRACT: Atomically thin two-dimensional (2D) semiconductors have presented a plethora of opportunities for future optoelectronic devices and photonics applications, made possible by the strong light matter interactions at the 2D quantum limit. Many body interactions between fundamental particles in 2D semiconductors are strongly enhanced compared with those in bulk semiconductors because of the reduced dimensionality and, thus, reduced dielectric screening. These enhanced many body interactions lead to the formation of robust quasi-particles, such as excitons, trions, and biexcitons, which are extremely important for the optoelectronics device applications of 2D semiconductors, such as light emitting diodes, lasers, and optical modulators, etc. Recently, the emerging anisotropic 2D semiconductors, such as black phosphorus (termed as phosphorene) and phosphorene-like 2D materials, such as ReSe₂, 2D-perovskites, SnS, etc., show strong anisotropic optical and electrical properties, which are different from conventional isotropic 2D semiconductors, such as transition metal dichalcogenide (TMD) monolayers. This anisotropy leads to the formation of quasi-one-dimensional (quasi-1D) excitons and trions in a 2D system, which results in even stronger many body interactions in anisotropic 2D materials, arising from the further reduced dimensionality of the quasi-particles and thus reduced dielectric screening. Many body interactions have been heavily investigated in TMD monolayers in past years, but not in anisotropic 2D materials yet. The quasi-particles in anisotropic 2D materials have fractional dimensionality which makes them perfect candidates to serve as a platform to study fundamental particle interactions in fractional dimensional space.



In this Account, we present our recent progress related to 2D phosphorene, a 2D system with quasi-1D excitons and trions. Phosphorene, because of its unique anisotropic properties, provides a unique 2D platform for investigating the dynamics of excitons, trions, and biexcitons in reduced dimensions and fundamental many body interactions. We begin by explaining the fundamental reasons for the highly enhanced interactions in the 2D systems influenced by dielectric screening, resulting in high binding energies of excitons and trions, which are supported by theoretical calculations and experimental observations. Phosphorene has shown much higher binding energies of excitons and trions than TMD monolayers, which allows robust quasi-particles in anisotropic materials at room temperature. We also discuss the role of extrinsic defects induced in phosphorene, resulting in localized excitonic emissions in the near-infrared range, making it suitable for optical telecommunication applications. Finally, we present our vision of the exciting device applications based on the highly enhanced many body interactions in phosphorene, including exciton-polariton devices, polariton lasers, single-photon emitters, and tunable light emitting diodes (LEDs).

1. INTRODUCTION

The discovery of graphene in 2004 opened avenues for a new generation of 2D materials. It was followed by exploration of other 2D semiconductor materials such as transition metal dichalcogenides (TMDs),^{1,2} phosphorene,³ etc. Stronger interaction within lower dimensional systems leads to existence of robust many-body systems^{2,4} and quasi-particles^{5,6} in these atomically thin layered materials. These quasi-particles have been shown to exist in quasi-2D systems (quantum wells),^{7,8} 2D materials,^{4,5,9} and 1D carbon nanotubes (CNTs).¹⁰ The strong interaction is measured by “binding energy” of these

quasi-particle systems. High binding energies allow these many body interactions between electrons and holes to be experimentally detected in various combined forms, such as excitons (electron and hole pair),¹¹ trions (charged excitons),¹² and biexciton (quantum combination of two-excitons: steady state or a trion and free charge: excited state).¹³ Binding energies of excitons (trions) have been theoretically and experimentally demonstrated to be in the range of 5–35 (1–5)

Received: October 9, 2017

Published: April 19, 2018

Table 1. Experimental and Theoretical Binding Energy Values (meV) for Various Quasi-Particles in Different Materials^a

system		quasi-2D	2D				anisotropic 2D				1D	
material		quantum wells	1L MoS ₂	1L MoSe ₂	1L WS ₂	1L WSe ₂	1L phosphorene	1L ReSe ₂	1L ReS ₂	1L GeS	1L GeSe	CNT
exciton	exp	8.7–9.2	550 ¹⁶	500 ¹⁶	660 ⁶	380 ¹⁶		860 ⁵⁴				410 1000
	theory	6.6–33.6	540 ¹⁵	470 ¹⁵	500 ¹⁵	450 ¹⁵	830 ³⁴	870 ⁵⁴	1070 ⁵⁶	1200 ⁵¹	400 ⁵¹	210–1100
trion	exp	1.1–5.5	18 ⁴	30 ⁵⁷	36 ⁵⁷	30 ³¹	162 ^{b24}					140–170
	theory	1.4–8.9	34 ⁵⁷	31 ⁵⁷	31 ⁵⁷	29 ⁵⁷	200 ²⁴					36–200
biexciton	exp	T + C	70 ⁵⁸	60 ¹³	65 ⁵⁹	52 ⁶⁰						130
		X + X										
	theory	T + C	2.13–2.24	69 ¹³	58 ¹³	67 ¹³	59 ¹³					40–56
	X + X		22 ⁵⁸	23 ⁵⁷	24 ⁵⁸	20 ⁵⁸	41 ³²					

^aNote: T is trion, C is charge, and X is exciton. This distinction has been made to identify excited state (T + C) and steady state (X + X) biexcitons. This distinction has not been made for biexciton values from quantum wells and CNT. References for binding energies of CNTs and quantum wells have been cited in-text because of the large number of references. ^bThe value is from 3L phosphorene sample.

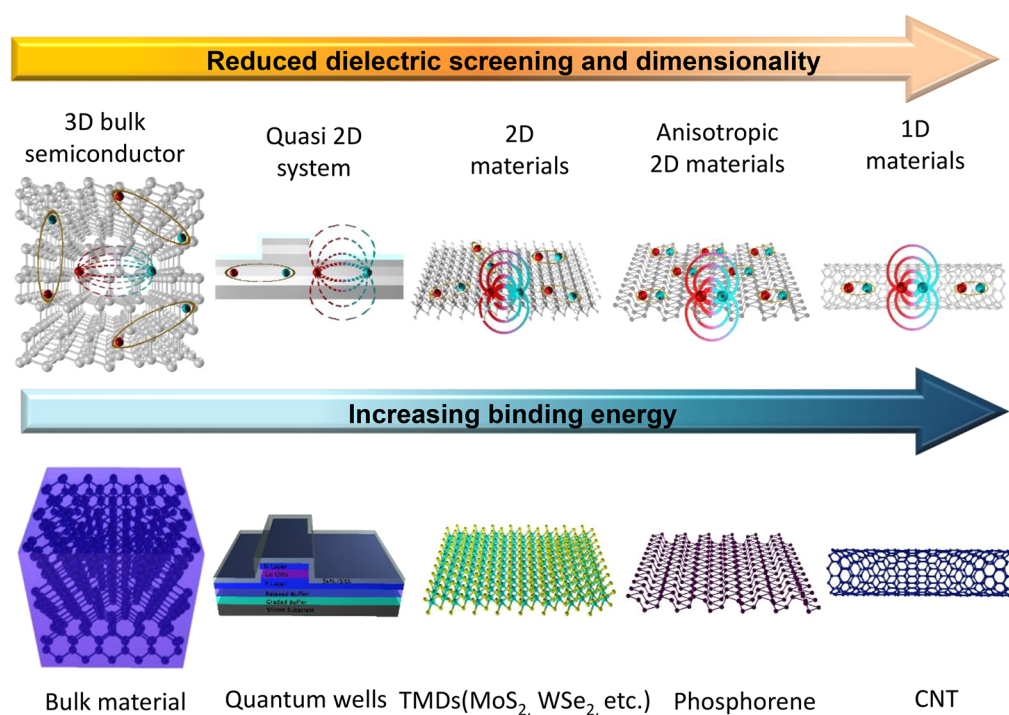


Figure 1. From 3D state (left) to truly 1D state (right) as the dimensionality decreases the dielectric screening decreases while the binding energy or the interaction of many body quasi-particles increases. In 3D state, electric field lines interacting between two fundamental particles are screened by the material. This screening reduces as the particles are further confined dimensionally in quantum wells (quasi-2D systems). 2D materials allow even stronger Coulombic interactions due to absence of any dielectric materials and results in even stronger in-plane many body systems spread across a single plane. In phosphorene, due to puckered configuration of the molecules the many body systems are confined along a quasi-1D space resulting in even higher interactions and binding energies, like a true 1D system, such as a CNT.

meV in quantum wells,¹⁴ 400–550 (20–34) meV in TMD monolayer,^{15,16} and 210–1100 (36–200) meV in CNTs.^{17–20} Detailed values of exciton, trion, and biexciton binding energies from various material systems from theoretical and experimental work have been summarized in Table 1.

However, the relatively low values of binding energies in quasi-2D and 2D systems only allow the exciton and trion photoluminescence (PL) peaks to segregate at cryogenic temperatures, barely resolvable at room temperature compared to their emission bandwidth.²¹ On the other hand, excitons and trions in 1D confined space (such as CNTs) exhibit much higher binding energies and the complete separation of exciton and trion PL peaks at room temperature because of further

dimensionality reduction and reduced screening.^{1,10} However, the utilization of 1D CNTs for practical optoelectronic applications is critically limited by their small cross-sectional area.²² It is extremely difficult to assemble large-sized and optically uniform films composed of CNTs because of the varied distribution of chirality and other issues such as conversion of homogeneous templates into long-chain CNTs at low temperatures.^{22,23} It has been a long-standing scientific challenge to optimize this trade-off between enhanced binding energies at confined dimensionalities and reduced cross-sectional areas, limiting the development of useful excitonic/trionic devices.

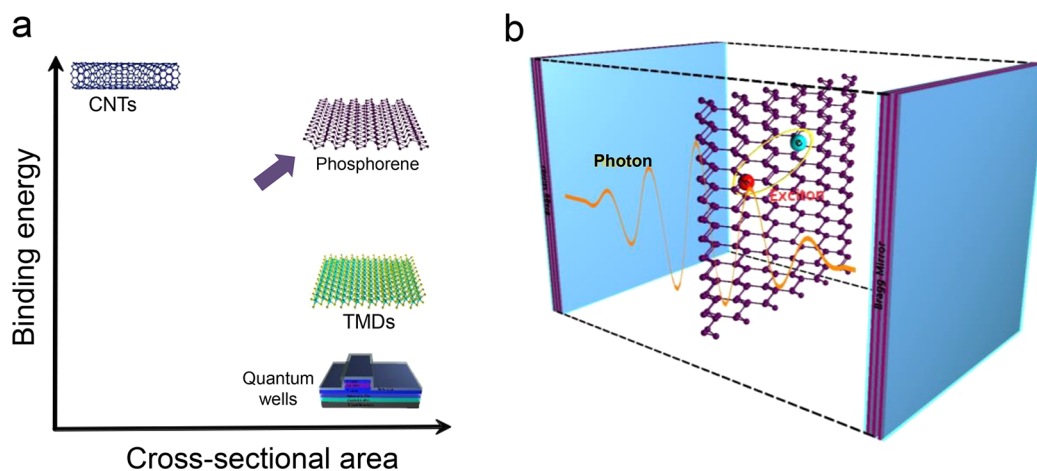


Figure 2. (a) Phosphorene provides high binding energies similar to a true 1D system with a large 2D cross-sectional area. (b) Schematic diagram of an exciton-polariton interaction in a cavity with 2D material.

The recently emerged anisotropic 2D materials, such as phosphorene, provides an elegant way to solve this challenge. Compared with other 2D materials, phosphorene shows strongly anisotropic properties, which results in quasi-1D excitons and trions in a 2D system.^{9,24,25} In this Account, we use the example of phosphorene to demonstrate the role of enhanced many body interactions in anisotropic 2D semiconductors, as compared to other 2D materials, such as TMDs. This enables a system that addresses the above-mentioned problem of the trade-off. High binding energies with large cross-section grant opportunities to use phosphorene in future optoelectronic devices, such as exciton-polariton devices, polariton lasers, tunable LEDs, and other excitonic devices based on exciton condensation.²⁶ This Account is directed toward highlighting the role of dimensional confinement and emphasizes on various experimental techniques employed by us and other groups to study these many body interactions and quasi particles. At the end, we present our visions and prospect on the potential optoelectronic applications of those anisotropic 2D materials.

2. EFFECT OF DIMENSIONALITY AND DIELECTRIC ENVIRONMENT ON FUNDAMENTAL QUASI-PARTICLES

Many body effects, which result from the Coulombic electron–hole interactions, play a key role in determining their electronic transport and optical properties.¹¹ The strength of electric fields between charged particles in a semiconducting material is determined by the level of Coulombic interaction between charged particles, which are affected by the dimensionality of the material and thus dielectric screening from the surrounding environment.²⁷ The effect of the dielectric environment on the interaction of charges and the binding energy in various dimensionalities of semiconductors have been represented schematically in Figure 1. In a conventional bulk semiconductor, the electron–holes interact with each other with electric field lines passing through the dielectric medium of the material itself, causing significant dielectric screening, resulting in weak interactions among the charges. Thus, the binding energy of these quasiparticle/many-body systems originating from the coulomb interaction is almost negligible. In quasi-2D quantum wells, the interaction enhances as the charges are only confined in a quasi-2D space and the dielectric screening is

diminished to an extent. In truly 2D materials, such as TMD monolayers, the dielectric screening to the interacting charges is considerably reduced due to the high localization of interacting charges within a single 2D plane²⁸ (Figure 1). The weak intrinsic screening results in enhanced many-body interactions at the 2D quantum limit. This effect is called the ‘dielectric confinement or “image-charge effect”’.¹ The stronger interaction leads to formation of stable excitons, trions, and biexcitons with higher binding energies as compared to quasi-2D systems. These quasi-particles have been demonstrated in various TMD materials, such as MoS₂,^{4,5} WS₂,^{2,6} MoSe₂,^{13,29} WSe₂^{30,31} with binding energies of excitons as high as ~0.6 eV and are stable at room temperature. Simultaneously, existence of robust charge interactions combined with dimensional confinement lead to formation of higher order excitonic complexes, such as trions⁴ and biexcitons.¹³ Compared with other 2D materials, phosphorene shows strongly anisotropic properties, which results in quasi-1D excitons and trions in the 2D phosphorene (Figure 1). Because of the formation of quasi-1D trions and excitons, 2D phosphorene has ultrahigh binding energies of excitons (~0.8 eV for monolayer phosphorene³²) and trions (~200 meV²⁴), much higher than those values in TMDs. As the dimensionality is further reduced to true 1D with advent of CNTs, the reported binding energies of excitons (>1 eV^{19,20}) and trions (~200 meV^{17,33}) were even higher than 2D systems due to further unidirectional confinement of charges.

However, high binding energies obtained from 1D CNTs are not applicable for widespread photonics devices applications due to the limited cross-section and difficulties in growing optically uniform integrated CNT networks.²² Phosphorene, due to its strong anisotropic optical and electrical properties,^{24,25} offers an alternative to solve aforementioned trade-off challenge. (Figure 2a). Phosphorene is equivalent to a system made from bundles of identical 1D semiconductors, allowing quasi-1D excitonic and trionic behavior in a large 2D area. This allows phosphorene’s optoelectronic integration for various unique applications in optoelectronics and quantum devices harnessing both the high excitonic and trionic binding energies and large cross-sectional area. For instance, phosphorene has promising applications in cavity devices such as exciton polariton devices (Figure 2b) operating at near-infrared (NIR) range, useful for telecommunication applications and integration with silicon photonics.

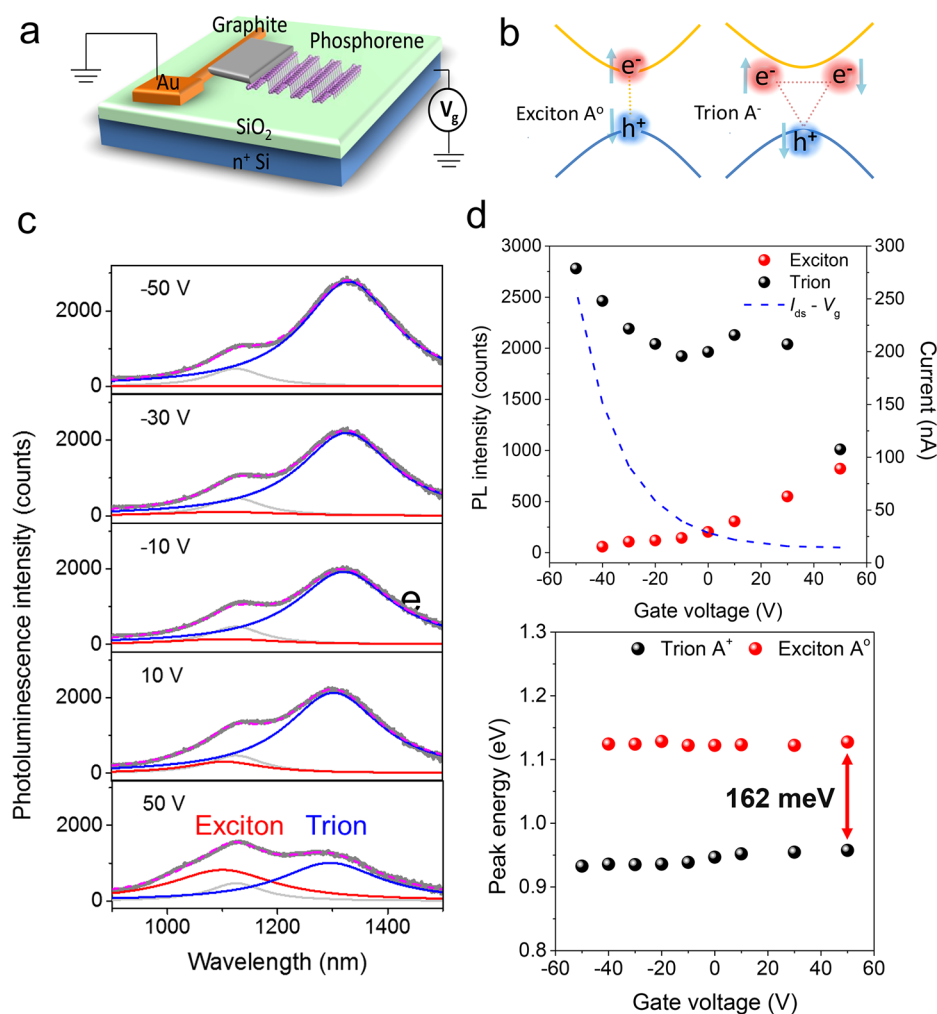


Figure 3. (a) Schematic diagram of the device used for exciton/trion modulation using external back gate voltage. (b) Schematic diagrams of excitons and trions. (c) PL intensity from 3L phosphorene as a function of back gate voltage. (d) Exciton and trion PL intensity variation with change in back gate voltage. (e) Variation in peak energies of exciton and trions as a function of back gate voltage. Figure 3 adapted with permission from ref 24. Copyright 2015 American Chemical Society.

3. TIGHTLY BOUND EXCITONS AND TRIONS IN PHOSPHORENE

Binding energy is the key parameter that defines the extent of interaction between fundamental particles.^{11,28} Several theoretical and experimental techniques have calculated the binding energy of excitons, trions and biexcitons. Table 1 summarizes the values of binding energies for various systems.

We successfully measured the binding energy of trions in a 3L phosphorene sample, using a metal-oxide-semiconductor (MOS) device to tune the PL emissions via controlling the electrostatic doping with applied back gate voltage, as shown in Figure 3a and b. The 3L phosphorene sample showed two emission peaks at ~ 1100 and ~ 1300 nm (Figure 3c–e), which were identified to be from excitons and trions, respectively. The relative intensity ratio of exciton/trion is tuned by gate voltage. When negative voltage is applied, positive charges are injected in to the sample and hence the trionic emissions dominated and vice versa. We also demonstrated that optical charge injection can also be controlled with excitation power, to tune the trion density in 1L phosphorene.²⁴ Therefore, binding energy of trions in 3L phosphorene was measured to be ~ 160 meV, which is much larger than those values in TMD

monolayers and is comparable to that in truly 1D CNTs (Table 1).

High-binding energy is attributed to anisotropic orientation of charged many body complexes in phosphorene, which has been theoretically predicted as well.³⁴ We, confirmed this anisotropic excitonic and trionic emission from phosphorene using angle resolved PL spectroscopy.^{9,24} The PL intensity is highly dependent on the polarization angle of the incident light due to anisotropic absorption in phosphorene attributed to its puckered structure. We also observed that emission of excitonic emissions from phosphorene was also linearly polarized sharply. Thus, the many body complexes are mostly aligned along the armchair direction (as shown in Figure 1). This strong anisotropy results in higher binding energies which can result in several photonics device applications, which will be discussed in the later section.

4. PRODUCING AIR-STABLE MONOLAYER PHOSPHORENE

Degradation of phosphorene has been a long-standing challenge for the scientific community. It is easily oxidized in the presence of oxygen, moisture, and light.³⁵ Several different passivation techniques have been demonstrated including,

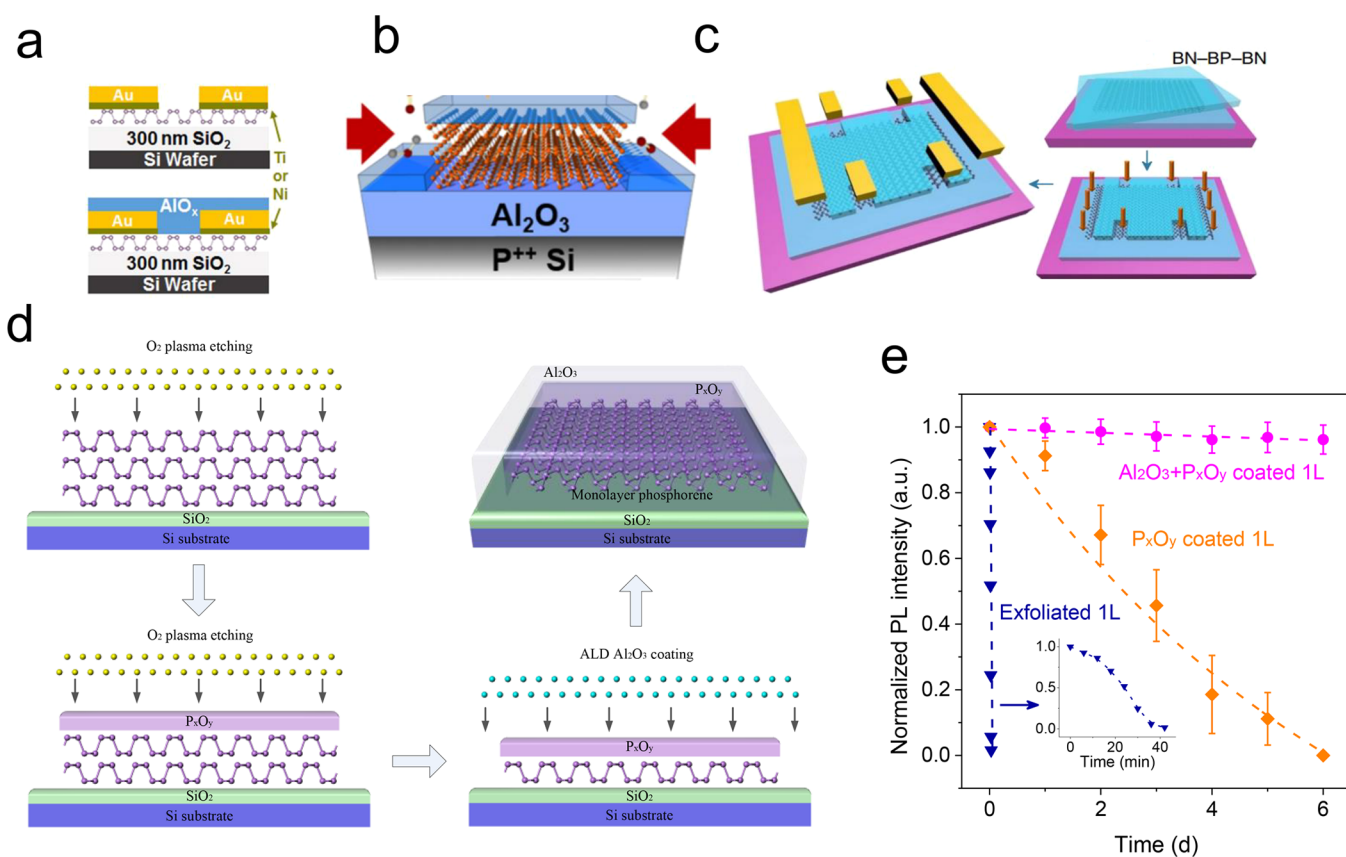


Figure 4. Schematic diagrams showing the passivation of phosphorene using (a) AlO_x , (b) Al_2O_3 , and (c), sandwiching between BN layers. Figure 4a adapted with permission from ref 36. Copyright 2014 American Chemical Society. Figure 4b adapted with permission from ref 37. Copyright 2015, Macmillan Publishers Limited. Figure 4c adapted with permission from ref 38. Copyright 2015 Macmillan Publishers Limited. (d) Passivation of few-layer phosphorene by combining the oxygen plasma treatment and Al_2O_3 encapsulation. (e) PL emission comparison from passivated and unpassivated phosphorene versus time. Panels d and e adapted with permission from ref 39. Copyright 2016 Nature Publishing group.

passivation through coating by Al_2O_3 ³⁶ by atomic layer deposition (ALD) technique³⁷ and sandwiching between h-BN layers³⁸ (Figure 4a–c). But, these techniques have been only partially successful in preserving fast degrading phosphorene flakes in the ambient environment.³⁹ The h-BN encapsulation requires very complicated technique and has a low-throughput. Recently, we developed a novel technique (Figure 4d) combining oxygen plasma etching with subsequent Al_2O_3 deposition to preserve phosphorene flakes in pristine condition in ambient environment. This method has 2-fold advantages. It allows for controlling the thickness of phosphorene very precisely and effective preservation of the phosphorene samples. Oxygen plasma is used to etch through a thick flake of phosphorene. During the treatment, top layers of phosphorene are oxidized to become P_xO_y , which serve as protecting layers for phosphorene underneath. Further plasma etching allows oxygen plasma to penetrate this P_xO_y layer and further oxidize the phosphorene layer underneath. After some time, a dynamic equilibrium is established so that etching rate and thickness of P_xO_y become constant. This allows precise etching down to monolayer. Finally, an additional layer of Al_2O_3 is deposited over the etched phosphorene and P_xO_y to protect it from oxidation. We found that mono- and bilayer samples which were fabricated by O_2 plasma etching can be coated with ALD Al_2O_3 without any further damage to the phosphorene samples under it due to the protective P_xO_y layer on top of it. This technique allows forming a controlled air-

stable few- to monolayered phosphorene samples, enabling its practical applicability in various device applications (Figure 4e).

5. DEFECT ENGINEERING IN PHOSPHORENE

Defect engineering in 2D materials has emerged a sturdy technique to modulate their optical properties for suitable optoelectronic applications. Single-photon emitters have been demonstrated from TMDs⁴⁰ and h-BN⁴¹ recently. The defect states can be realized through oxidation, irradiation, and physical absorption.⁴² Phosphorene and other similar structure based anisotropic materials (ReS_2 , and ReSe_2) offer a distinct advantage for defect engineering due to their puckered sp^3 -like configuration. Defect induction in phosphorene is critical for triggering photon emission at new wavelengths, utilizing the layer dependent band gap in phosphorene from future optoelectronic devices point of view.

We induced defects in monolayer phosphorene using two distinctive methods.^{39,42} First, we used a plasma-enhanced chemical vapor deposition (PECVD) oxide substrate and deposited gold over it followed by phosphorene. PECVD oxide contained a lot of impurities and surface states, which were confirmed with FTIR spectroscopy. These surface states then act as trapping centers for excitons.²¹ Second, we introduced extrinsic oxygen defects in monolayer phosphorene using external oxygen plasma etching.³⁹ Extrinsic defects as dangling “O” bonds are quite common in phosphorene and have been discussed in literature.⁴³ Another form is the diagonal oxygen bridge (Figure 5a), which acts as potential trap state and is

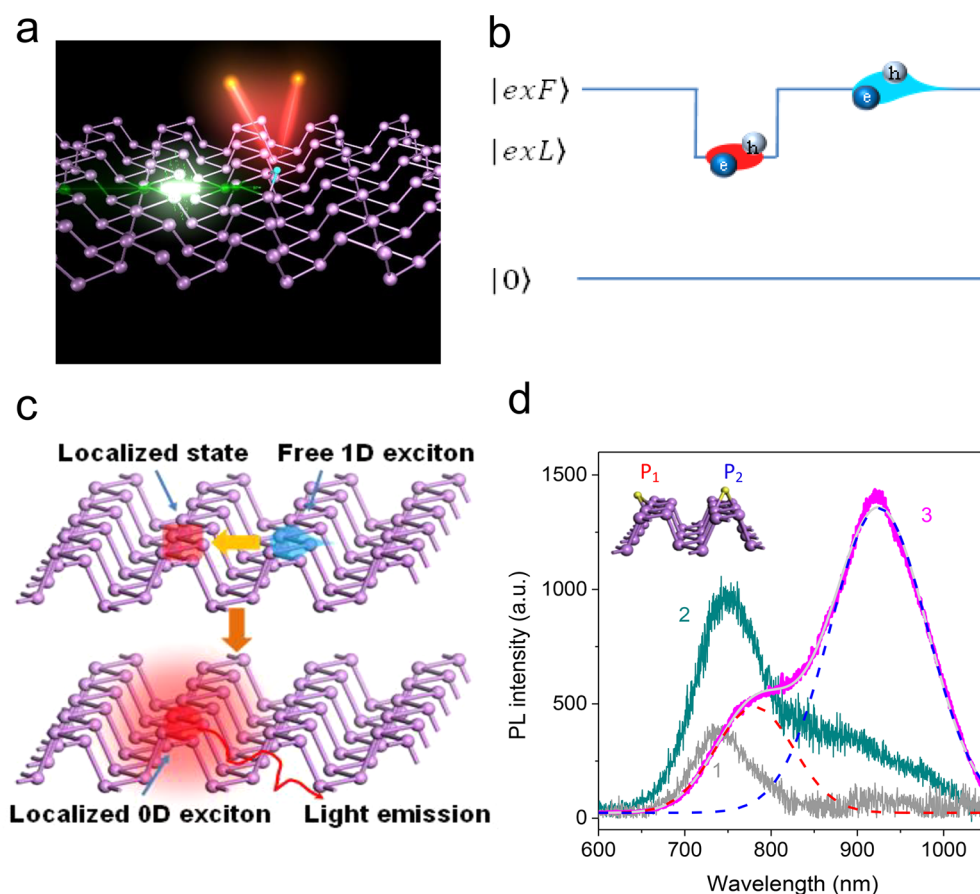


Figure 5. (a) Schematic diagram showing the defect emission from a diagonal bridge type defect in phosphorene. (b, c) Schematic showing the formation of lower energy defect states in phosphorene with respect to the free excitonic energy levels. (d) PL emission from defect engineered phosphorene monolayer with defect shown inset. The green curve represents the free excitonic emission from untreated graphene. The pink curve represents the free and localized excitonic emission from oxygen plasma treated graphene. The dotted curves are Lorentzian fit curves. Figures 5b and c are adapted with permission from ref 42. Copyright 2016 Wiley. Figure 5d adapted from ref 39. Copyright 2016 Nature Publishing group.

quite stable. These surface defects can alter the optical properties of phosphorene and result in defect levels being created in the optical band gap of the materials (Figure 5b), which causes excitonic emissions from these localized states at lower energies than free exciton emission energies (Figure 5c). For defect engineering in monolayer phosphorene, we observed a free exciton emission at ~ 720 nm attributed to the free excitonic emission and low energy emission at ~ 920 nm (Figure 5d). The defect peak shows a sublinear growth in the integrated PL emission with increasing excitation laser power, thus establishing its defect nature.³⁹ The defect emission peaks were observed at room temperature, which is in contrast with defect emissions from TMDs that are only visible at cryogenic temperatures.²¹ The localized excitonic emissions at 920 nm showed much higher PL emission efficiency as compared to the free excitonic state. The overall quantum efficiency was extracted to be ~ 33.6 times higher than free excitonic emission.⁴² The enhanced PL emission yield could be attributed to the longer lifetime-radiative recombination of localized excitons in the trapping states. The defect states can function as quasi-zero-dimensional (quasi-0D) luminescence trapping centers with enhanced PL emission efficiencies. 2D phosphorene, with quasi-1D free excitons and quasi-0D localized excitons forms an interesting 2D–1D–0D hybrid system, which provides us a unique platform to explore the fundamental interactions at multidimensionalities.⁴² As sug-

gested earlier, anisotropic materials due their specific molecular orientation are ideal candidates for defect engineering using any of the above-mentioned techniques. This is particularly interesting for phosphorene due to its layer dependent band gap, it could possibly lead to defect emissions in the infrared range. Most defect emissions in other TMDs and 1L phosphorene are >1 eV, which is in the visible range. Few-layered phosphorene samples can trigger emissions at much lower energies that are useful for telecommunication device applications.⁴⁴

6. OUR VISION: DEVICES BASED ON STRONG LIGHT MATTER INTERACTIONS IN PHOSPHORENE

The enhanced binding energies of these quasi-particles as discussed earlier is crucial for promising device applications. In this section, we will present our vision for such optoelectronic devices and their working principles based on phosphorene and other similar anisotropic 2D materials. Figure 6a depicts the key domains of device applications based on phosphorene directly linked with the interesting properties we have discussed earlier in this account. For example, high binding energy allows for its integration into a microcavity for electronically pumped exciton-polariton lasers.

In microcavities created by Bragg's mirror on either side of the 2D material (Figure 2b), a strong coupling of excitons and optical fields can be generated. 2D excitons and 2D optical

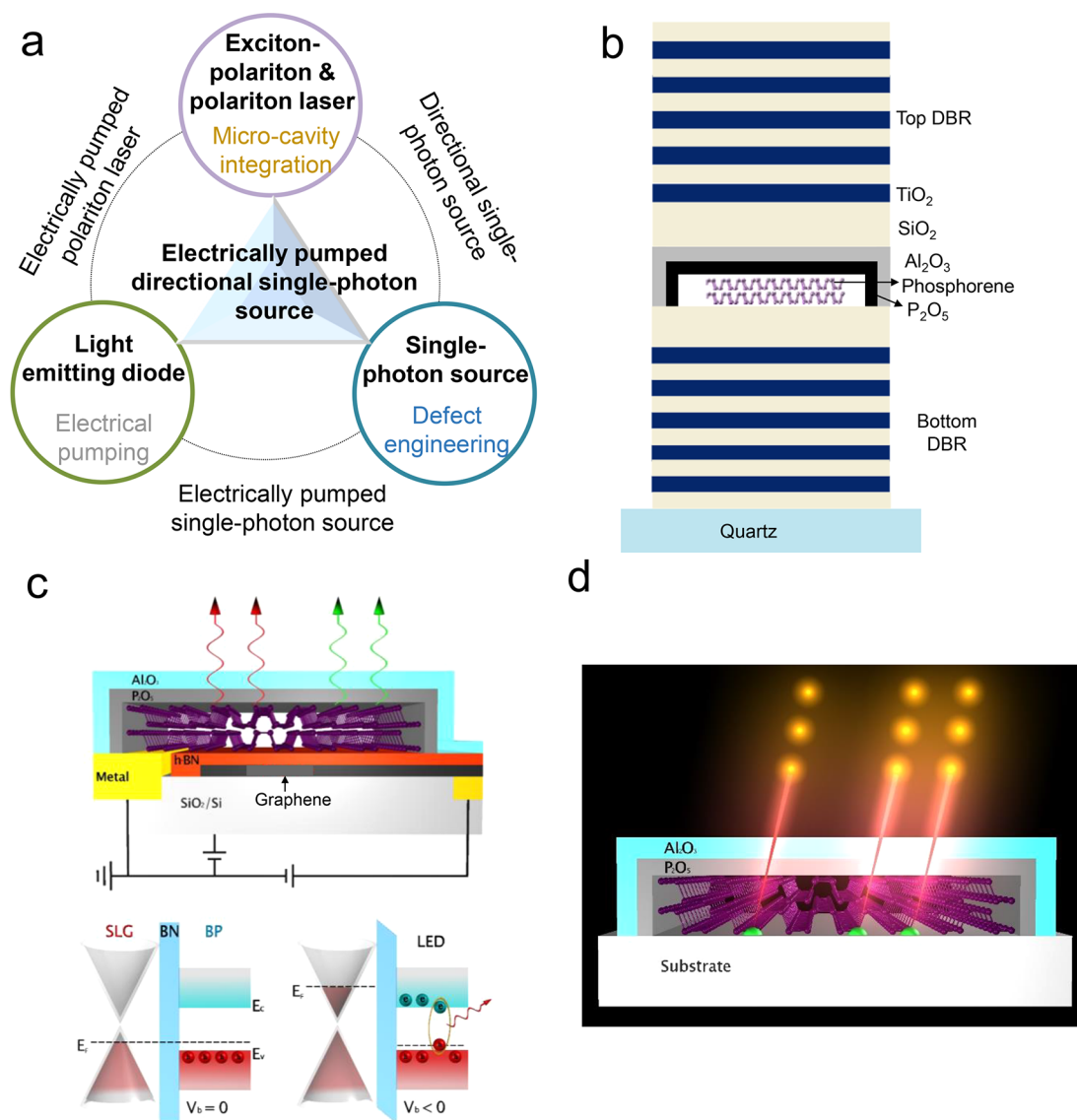


Figure 6. (a) Envisioned research domains with anisotropic materials. (b) Schematic of the structure of planar microcavity composed of dual DBRs with the embedded phosphorene. (c) Schematic plot of the tunable phosphorene LED. Heterostructure band diagram shows the case for zero-bias and the case for a finite negative bias applied to the single layer graphene (SLG). BP: phosphorene. (d) Schematic diagram showing single-photon emissions from defect states in phosphorene.

modes in the strong coupling regime in these cavities gives rise to new eigenmodes called excitons-polaritons.⁴⁵ These can enable study of quantum phenomenon such as Bose–Einstein condensation, quantum vortices, and entangled photon pairs.⁴⁶ Earlier reported exciton-polaritons have been based on quantum wells, where these quasi-particles were only visible at cryogenic temperatures. Recently, they have been reported with TMD based materials⁴⁵ in the microcavities owing to their strong binding energy and direct band gap nature. Exciton-polariton devices operating the infrared region are critical for telecommunication applications and integration with conventional silicon photonics. Recently, NIR exciton-polaritons were reported using single walled CNTs.²² But, CNT-based devices show large performance variation, since it is difficult to control the position, alignment and chirality of the CNTs in the cavity as discussed earlier. Phosphorene thus, provides a high binding energy system, stable, perfectly controllable platform to demonstrate such devices working the NIR region. Layer-dependent band gap⁹ of phosphorene also allows flexibility of

choosing the emission wavelength range. As shown in the Figure 6b, the microcavity consists of atomically thin phosphorene sandwiched between two SiO_2 layers, which is placed between $\text{SiO}_2/\text{TiO}_2$ distributed Bragg's Reflector (DBR) mirrors. The cavity resonance can be controlled to match well with exciton energy emitting from phosphorene sample. Polariton lasers⁴⁷ can be made using the stimulated scattering from exciton-polaritons that promises more energy efficient generation of coherent light.⁴⁸ The threshold energy for coherent emission from a phosphorene polariton laser will be much smaller as compared to a conventional laser.

Simultaneously, light emitting junctions based on TMD materials have been demonstrated including the lateral p – n junctions, vertical heterojunction diodes⁴⁹ and vertical tunneling transistors.⁵⁰ But, their emission wavelength as stated above remains confined in the visible region. Phosphorene based LEDs (Figure 6c) can act as potential sources for NIR and even middle infrared (MIR) region emission for telecommunication applications. Also, as we have demonstrated

earlier excitonic and trionic emissions from phosphorene can be controlled using external back gate tuning.²⁴ Thus, phosphorene can enable tunable wavelength emissions from a single device, by controlling the back-gate voltage as shown in the schematic diagram Figure 6c. A vertically stacked heterojunction with graphene and phosphorene allows for electroluminescence (EL) from the whole device area, unlike Schottky junction or split-gate $p-n$ junction devices providing the benefit of atomically precise interfaces and barrier thickness.

Defect engineering in phosphorene as discussed earlier can lead to potential device applications.⁴² These defects act as efficient trapping centers, which when isolated can act as sources of single-photon emission. 2D materials have several key advantages to host single-photon emitters as they can negate the total internal reflection enabling high light extraction efficiency, enabling integration with photonic waveguides and plasmonic structures. They have been demonstrated recently with h-BN and TMD materials⁴¹ in which quantum defects are ascribed to localized excitons. But, for all single-photon emitters demonstrated in TMDs and h-BN operate in the visible range, limiting their application to quantum communication systems based on NIR fiber transmission. As we have demonstrated in our previous reports,^{39,42} defects can be implanted in phosphorene enabling low energy defect states by either substrate engineering or external oxygen plasma etching. PL emission from phosphorene can be tuned using defect integration with few layer phosphorene. Thus, making phosphorene few layers as an ideal host for single-photon emitters in NIR wavelength (Figure 6d). These defect emissions are in sharp contrast with defect emissions from TMDs, which are only visible at cryogenic temperatures.²¹ The defect emission from these defect/localized states is brighter (higher quantum efficiency) as compared to the free excitonic emission making it more suitable for NIR and MIR single-photon emission-based devices.

7. OTHER ANISOTROPIC MATERIALS

Apart from phosphorene, other anisotropic materials like GeSe/GeS,⁵¹ SnS,⁵² SnSe,⁵³ ReSe₂, ReS₂,⁵⁴ and 2D perovskites⁵⁵ have also shown strong anisotropic optical properties. The theoretically calculated binding energies of the various fundamental quasi-particles are similar to those in phosphorene (Table 1), making them suitable for all the above-mentioned applications. Also, they are made of earth abundant and environmentally friendly elements making them suitable for optoelectronic applications.

8. CONCLUSIONS AND PROSPECTS

The ability to fabricate materials that are atomically thin has led us to explore stronger light-matter interaction that exist at that level. While reflecting on the key reasons for such strong interactions at the 2D limit, we highlighted the role of these interactions in enabling us to study the properties and applications of the quasi-particles such as excitons and trions in this account. Using our recent experimental observations on phosphorene, we highlight the importance of such anisotropic 2D semiconductors that provide a quasi-1D platform in a 2D system enabling even higher binding energies of excitons and trions. First, we calculated exciton and trion binding energies in phosphorene, which is one-order higher as compared to other TMD materials. Higher excitonic/trionic interactions in a quasi-1D anisotropic material enable exciting device applica-

tions, such as exciton-polariton lasers and tunable LEDs. Degradation of phosphorene has been a major deterrent for its broad application. We discussed one of our recently developed technique to precisely thin down the thickness of phosphorene few layers and passivate it using Al₂O₃ simultaneously. Simultaneously, we described the role of defect engineered emissions from phosphorene, which can be used to demonstrate single-photon emitters from phosphorene working in the infrared range. Compared to other 2D materials, defect emissions from anisotropic materials are more stable at room temperature. We envision similar techniques that we have described can be extended to other anisotropic materials, such as ReSe₂, ReS₂, GeS, GeSe₂, and 2D perovskites to explore interesting and even stronger light matter interactions at the 2D limit enabling various optoelectronic and photonics device applications.

AUTHOR INFORMATION

Corresponding Author

*E-mail: yuerui.lu@anu.edu.au.

ORCID

Ankur Sharma: 0000-0002-0863-1857

Yuerui Lu: 0000-0001-6131-3906

Notes

The authors declare no competing financial interest.

Biographies

Ankur Sharma is a Ph.D. student at NEMS lab in Australian National University (ANU). His research interests include 2D materials and device fabrication based on 2D materials.

Han Yan is a third-year undergraduate student at Research School of Engineering, ANU.

Linglong Zhang is a Ph.D. student at Nanjing University, China, and a visiting PhD research student at Australian National University.

Xueqian Sun is a postgraduate student at ANU.

Boqing Liu is a postgraduate student in NEMS lab in ANU.

Dr. Yuerui Lu is an Associate Professor and group leader of Nanoelectro-mechanical System (NEMS) Lab at ANU. His research interests include MEMS/NEMS, nanomanufacturing, renewable energy harvesting, biomedical novel devices, and 2D materials.

REFERENCES

- (1) Chernikov, A.; Berkelbach, T. C.; Hill, H. M.; Rigosi, A.; Li, Y.; Aslan, O. B.; Reichman, D. R.; Hybertsen, M. S.; Heinz, T. F. Exciton binding energy and nonhydrogenic Rydberg series in monolayer WS₂. *Phys. Rev. Lett.* **2014**, *113*, 076802.
- (2) Hill, H. M.; Rigosi, A. F.; Roquelet, C.; Chernikov, A.; Berkelbach, T. C.; Reichman, D. R.; Hybertsen, M. S.; Brus, L. E.; Heinz, T. F. Observation of excitonic Rydberg states in monolayer MoS₂ and WS₂ by photoluminescence excitation spectroscopy. *Nano Lett.* **2015**, *15*, 2992–2997.
- (3) Ling, X.; Wang, H.; Huang, S.; Xia, F.; Dresselhaus, M. S. The renaissance of black phosphorus. *Proc. Natl. Acad. Sci. U. S. A.* **2015**, *112*, 4523–4530.
- (4) Mak, K. F.; He, K.; Lee, C.; Lee, G. H.; Hone, J.; Heinz, T. F.; Shan, J. Tightly bound trions in monolayer MoS₂. *Nat. Mater.* **2013**, *12*, 207–211.
- (5) Lin, Y.; Ling, X.; Yu, L.; Huang, S.; Hsu, A. L.; Lee, Y.-H.; Kong, J.; Dresselhaus, M. S.; Palacios, T. Dielectric screening of excitons and trions in single-layer MoS₂. *Nano Lett.* **2014**, *14*, 5569–5576.

- (6) Ye, Z.; Cao, T.; O'Brien, K.; Zhu, H.; Yin, X.; Wang, Y.; Louie, S. G.; Zhang, X. Probing excitonic dark states in single-layer tungsten disulphide. *Nature* **2014**, *513*, 214–218.
- (7) Kheng, K.; Cox, R.; d'Aubigné, M. Y.; Bassani, F.; Saminadayar, K.; Tatarenko, S. Observation of negatively charged excitons X⁻ in semiconductor quantum wells. *Phys. Rev. Lett.* **1993**, *71*, 1752.
- (8) Mathieu, H.; Lefebvre, P.; Christol, P. Simple analytical method for calculating exciton binding energies in semiconductor quantum wells. *Phys. Rev. B: Condens. Matter Mater. Phys.* **1992**, *46*, 4092.
- (9) Zhang, S.; Yang, J.; Xu, R.; Wang, F.; Li, W.; Ghufraan, M.; Zhang, Y.-W.; Yu, Z.; Zhang, G.; Qin, Q.; Lu, Y. Extraordinary Photoluminescence and Strong Temperature/Angle-Dependent Raman Responses in Few-Layer Phosphorene. *ACS Nano* **2014**, *8*, 9590–9596.
- (10) Brozena, A. H.; Leeds, J. D.; Zhang, Y.; Fourkas, J. T.; Wang, Y. Controlled Defects in Semiconducting Carbon Nanotubes Promote Efficient Generation and Luminescence of Trions. *ACS Nano* **2014**, *8*, 4239–4247.
- (11) Rodin, A.; Carvalho, A.; Castro Neto, A. H. Excitons in anisotropic two-dimensional semiconducting crystals. *Phys. Rev. B: Condens. Matter Mater. Phys.* **2014**, *90*, 075429.
- (12) Thilagam, A. Two-dimensional charged-exciton complexes. *Phys. Rev. B: Condens. Matter Mater. Phys.* **1997**, *55*, 7804.
- (13) Pei, J.; Yang, J.; Wang, X.; Wang, F.; Mokkaapati, S.; Lü, T.; Zheng, J.-C.; Qin, Q.; Neshev, D.; Tan, H. H.; Jagadish, C.; Lu, Y. Excited State Biexcitons in Atomically Thin MoSe₂. *ACS Nano* **2017**, *11*, 7468–7475.
- (14) Schulz, S.; O'Reilly, E. P. Excitonic binding energies in non-polar GaN quantum wells. *Phys. Status Solidi C* **2010**, *7*, 1900–1902.
- (15) Berkelbach, T. C.; Hybertsen, M. S.; Reichman, D. R. Theory of neutral and charged excitons in monolayer transition metal dichalcogenides. *Phys. Rev. B: Condens. Matter Mater. Phys.* **2013**, *88*, 045318.
- (16) Rasmussen, F. A.; Thygesen, K. S. Computational 2D materials database: electronic structure of transition-metal dichalcogenides and oxides. *J. Phys. Chem. C* **2015**, *119*, 13169–13183.
- (17) Kammerlander, D.; Prezzi, D.; Goldoni, G.; Molinari, E.; Hohenester, U. Biexciton stability in carbon nanotubes. *Phys. Rev. Lett.* **2007**, *99*, 126806.
- (18) Liang, S.; Ma, Z.; Wei, N.; Liu, H.; Wang, S.; Peng, L. M. Solid state carbon nanotube device for controllable trion electroluminescence emission. *Nanoscale* **2016**, *8*, 6761–9.
- (19) Ma, Y.-Z.; Valkunas, L.; Bachilo, S. M.; Fleming, G. R. Exciton binding energy in semiconducting single-walled carbon nanotubes. *J. Phys. Chem. B* **2005**, *109*, 15671–15674.
- (20) Maultzsch, J.; Pomraenke, R.; Reich, S.; Chang, E.; Prezzi, D.; Ruini, A.; Molinari, E.; Strano, M. S.; Thomsen, C.; Lienau, C. Exciton binding energies in carbon nanotubes from two-photon photoluminescence. *Phys. Rev. B: Condens. Matter Mater. Phys.* **2005**, *72*, 241402.
- (21) Tongay, S.; Suh, J.; Ataca, C.; Fan, W.; Luce, A.; Kang, J. S.; Liu, J.; Ko, C.; Raghunathan, R.; Zhou, J.; Ogletree, F.; Li, J.; Grossman, J. C.; Wu, J. Defects activated photoluminescence in two-dimensional semiconductors: interplay between bound, charged, and free excitons. *Sci. Rep.* **2013**, *3*, 2657.
- (22) Graf, A.; Tropic, L.; Zakharko, Y.; Zaumseil, J.; Gather, M. C. Near-infrared exciton-polaritons in strongly coupled single-walled carbon nanotube microcavities. *Nat. Commun.* **2016**, *7*, 13078.
- (23) Jasti, R.; Bertozzi, C. R. Progress and Challenges for the Bottom-Up Synthesis of Carbon Nanotubes with Discrete Chirality. *Chem. Phys. Lett.* **2010**, *494*, 1–7.
- (24) Xu, R.; Zhang, S.; Wang, F.; Yang, J.; Wang, Z.; Pei, J.; Myint, Y. W.; Xing, B.; Yu, Z.; Fu, L.; Qin, Q.; Lu, Y. Extraordinarily bound quasi-one-dimensional trions in two-dimensional phosphorene atomic semiconductors. *ACS Nano* **2016**, *10*, 2046–2053.
- (25) Yang, J.; Xu, R.; Pei, J.; Myint, Y. W.; Wang, F.; Wang, Z.; Zhang, S.; Yu, Z.; Lu, Y. Optical tuning of exciton and trion emissions in monolayer phosphorene. *Light: Sci. Appl.* **2015**, *4*, e312.
- (26) High, A. A.; Novitskaya, E. E.; Butov, L. V.; Hanson, M.; Gossard, A. C. Control of exciton fluxes in an excitonic integrated circuit. *Science* **2008**, *321*, 229–231.
- (27) Wang, Y.; Zhang, S.; Huang, D.; Cheng, J.; Li, Y.; Wu, S. Screening effect of graphite and bilayer graphene on excitons in MoSe₂ monolayer. *2D Mater.* **2017**, *4*, 015021.
- (28) Thilagam, A. Exciton complexes in low dimensional transition metal dichalcogenides. *J. Appl. Phys.* **2014**, *116*, 053523.
- (29) Ross, J. S.; Wu, S.; Yu, H.; Ghimire, N. J.; Jones, A. M.; Aivazian, G.; Yan, J.; Mandrus, D. G.; Xiao, D.; Yao, W.; Xu, X. Electrical control of neutral and charged excitons in a monolayer semiconductor. *Nat. Commun.* **2013**, *4*, 1474.
- (30) He, K.; Kumar, N.; Zhao, L.; Wang, Z.; Mak, K. F.; Zhao, H.; Shan, J. Tightly bound excitons in monolayer WSe₂. *Phys. Rev. Lett.* **2014**, *113*, 026803.
- (31) Liu, H.; Jiao, L.; Xie, L.; Yang, F.; Chen, J.; Ho, W.; Gao, C.; Jia, J.; Cui, X.; Xie, M. Molecular-beam epitaxy of monolayer and bilayer WSe₂: a scanning tunneling microscopy/spectroscopy study and deduction of exciton binding energy. *2D Mater.* **2015**, *2*, 034004.
- (32) Chaves, A.; Mayers, M. Z.; Peeters, F. M.; Reichman, D. R. Theoretical investigation of electron-hole complexes in anisotropic two-dimensional materials. *Phys. Rev. B: Condens. Matter Mater. Phys.* **2016**, *93*, 115314.
- (33) Yoshida, M.; Popert, A.; Kato, Y. K. Gate-voltage induced trions in suspended carbon nanotubes. *Phys. Rev. B: Condens. Matter Mater. Phys.* **2016**, *93*, 041402.
- (34) Seixas, L.; Rodin, A. S.; Carvalho, A.; Castro Neto, A. H. Exciton binding energies and luminescence of phosphorene under pressure. *Phys. Rev. B: Condens. Matter Mater. Phys.* **2015**, *91*, 115437.
- (35) Favron, A.; Gaufres, E.; Fossard, F.; Phaneuf-L'Heureux, A.-L.; Tang, N. Y. W.; Levesque, P. L.; Loiseau, A.; Leonelli, R.; Francoeur, S.; Martel, R. Photooxidation and quantum confinement effects in exfoliated black phosphorus. *Nat. Mater.* **2015**, *14*, 826–832.
- (36) Wood, J. D.; Wells, S. A.; Jariwala, D.; Chen, K.-S.; Cho, E.; Sangwan, V. K.; Liu, X.; Lauhon, L. J.; Marks, T. J.; Hersam, M. C. Effective passivation of exfoliated black phosphorus transistors against ambient degradation. *Nano Lett.* **2014**, *14*, 6964–6970.
- (37) Kim, J.-S.; Liu, Y.; Zhu, W.; Kim, S.; Wu, D.; Tao, L.; Dodabalapur, A.; Lai, K.; Akinwande, D. Toward air-stable multilayer phosphorene thin-films and transistors. *Sci. Rep.* **2015**, *5*, 8989.
- (38) Chen, X.; Wu, Y.; Wu, Z.; Han, Y.; Xu, S.; Wang, L.; Ye, W.; Han, T.; He, Y.; Cai, Y.; Wang, N. High-quality sandwiched black phosphorus heterostructure and its quantum oscillations. *Nat. Commun.* **2015**, *6*, 7315.
- (39) Pei, J.; Gai, X.; Yang, J.; Wang, X.; Yu, Z.; Choi, D.-Y.; Luther-Davies, B.; Lu, Y. Producing air-stable monolayers of phosphorene and their defect engineering. *Nat. Commun.* **2016**, *7*, 10450.
- (40) Lin, Z.; Carvalho, B. R.; Kahn, E.; Lv, R.; Rao, R.; Terrones, H.; Pimenta, M. A.; Terrones, M. Defect engineering of two-dimensional transition metal dichalcogenides. *2D Mater.* **2016**, *3*, 022002.
- (41) Aharonovich, I.; Englund, D.; Toth, M. Solid-state single-photon emitters. *Nat. Photonics* **2016**, *10*, 631–641.
- (42) Xu, R.; Yang, J.; Myint, Y. W.; Pei, J.; Yan, H.; Wang, F.; Lu, Y. Exciton brightening in monolayer phosphorene via dimensionality modification. *Adv. Mater.* **2016**, *28*, 3493–3498.
- (43) Carvalho, A.; Wang, M.; Zhu, X.; Rodin, A. S.; Su, H.; Castro Neto, A. H. Phosphorene: from theory to applications. *Nature Reviews Materials* **2016**, *1*, 16061.
- (44) Qiao, J.; Kong, X.; Hu, Z.-X.; Yang, F.; Ji, W. High-mobility transport anisotropy and linear dichroism in few-layer black phosphorus. *Nat. Commun.* **2014**, *5*, 4475.
- (45) Liu, X.; Galfsky, T.; Sun, Z.; Xia, F.; Lin, E.-c.; Lee, Y.-H.; Kéna-Cohen, S.; Menon, V. M. Strong light–matter coupling in two-dimensional atomic crystals. *Nat. Photonics* **2015**, *9*, 30–34.
- (46) Bhattacharya, P.; Xiao, B.; Das, A.; Bhowmick, S.; Heo, J. Solid State Electrically Injected Exciton-Polariton Laser. *Phys. Rev. Lett.* **2013**, *110*, 206403.
- (47) Schneider, C.; Rahimi-Iman, A.; Kim, N. Y.; Fischer, J.; Savenko, I. G.; Amthor, M.; Lerner, M.; Wolf, A.; Worschech, L.; Kulakovskii,

V. D.; Shelykh, I. A.; Kamp, M.; Reitzenstein, S.; Forchel, A.; Yamamoto, Y.; Hofling, S. An electrically pumped polariton laser. *Nature* **2013**, *497*, 348–352.

(48) Tsintzos, S. I.; Pelekanos, N. T.; Konstantinidis, G.; Hatzopoulos, Z.; Savvidis, P. G. A GaAs polariton light-emitting diode operating near room temperature. *Nature* **2008**, *453*, 372–375.

(49) Withers, F.; Del Pozo-Zamudio, O.; Mishchenko, A.; Rooney, A. P.; Gholinia, A.; Watanabe, K.; Taniguchi, T.; Haigh, S. J.; Geim, A. K.; Tartakovskii, A. I.; Novoselov, K. S. Light-emitting diodes by band-structure engineering in van der Waals heterostructures. *Nat. Mater.* **2015**, *14*, 301–306.

(50) Ross, J. S.; Klement, P.; Jones, A. M.; Ghimire, N. J.; Yan, J.; Mandrus, D. G.; Taniguchi, T.; Watanabe, K.; Kitamura, K.; Yao, W.; Cobden, D. H.; Xu, X. Electrically tunable excitonic light-emitting diodes based on monolayer WSe₂ p–n junctions. *Nat. Nanotechnol.* **2014**, *9*, 268–272.

(51) Gomes, L. C.; Trevisanutto, P.; Carvalho, A.; Rodin, A.; Castro Neto, A. H. Strongly bound Mott-Wannier excitons in GeS and GeSe monolayers. *Phys. Rev. B: Condens. Matter Mater. Phys.* **2016**, *94*, 155428.

(52) Xia, J.; Li, X.-Z.; Huang, X.; Mao, N.; Zhu, D.-D.; Wang, L.; Xu, H.; Meng, X.-M. Physical vapor deposition synthesis of two-dimensional orthorhombic SnS flakes with strong angle/temperature-dependent Raman responses. *Nanoscale* **2016**, *8*, 2063–2070.

(53) Li, L.; Chen, Z.; Hu, Y.; Wang, X.; Zhang, T.; Chen, W.; Wang, Q. Single-layer single-crystalline SnSe nanosheets. *J. Am. Chem. Soc.* **2013**, *135*, 1213–1216.

(54) Arora, A.; Noky, J.; Druppel, M.; Jariwala, B.; Deilmann, T.; Schneider, R.; Schmidt, R.; Del Pozo-Zamudio, O.; Stiehm, T.; Bhattacharya, A.; Kruger, P.; Michaelis de Vasconcellos, S.; Rohlfing, M.; Bratschkitsch, R. Highly Anisotropic in-Plane Excitons in Atomically Thin and Bulklike 1T'-ReSe₂. *Nano Lett.* **2017**, *17*, 3202–3207.

(55) Stoumpos, C. C.; Malliakas, C. D.; Kanatzidis, M. G. Semiconducting tin and lead iodide perovskites with organic cations: phase transitions, high mobilities, and near-infrared photoluminescent properties. *Inorg. Chem.* **2013**, *52*, 9019–9038.

(56) Zhong, H.-X.; Gao, S.; Shi, J.-J.; Yang, L. Quasiparticle band gaps, excitonic effects, and anisotropic optical properties of the monolayer distorted 1 T diamond-chain structures ReS₂ and ReSe₂. *Phys. Rev. B: Condens. Matter Mater. Phys.* **2015**, *92*, 115438.

(57) Szyniszewski, M.; Mostaani, E.; Drummond, N. D.; Fal'ko, V. I. Binding energies of trions and biexcitons in two-dimensional semiconductors from diffusion quantum Monte Carlo calculations. *Phys. Rev. B: Condens. Matter Mater. Phys.* **2017**, *95*, 081301.

(58) Zhang, D. K.; Kidd, D. W.; Varga, K. The biexciton puzzle. 2015, arXiv1507.07858. aXiv.org e-Print archive. <https://arxiv.org/abs/1507.07858>.

(59) Plechinger, G.; Nagler, P.; Kraus, J.; Paradiso, N.; Strunk, C.; Schüller, C.; Korn, T. Identification of excitons, trions and biexcitons in single-layer WS₂. *Phys. Status Solidi RRL* **2015**, *9*, 457–461.

(60) You, Y.; Zhang, X.-X.; Berkelbach, T. C.; Hybertsen, M. S.; Reichman, D. R.; Heinz, T. F. Observation of biexcitons in monolayer WSe₂. *Nat. Phys.* **2015**, *11*, 477.